Tunable negligible-loss energy transfer between dipolar-coupled magnetic disks by stimulated vortex gyration

Hyunsung Jung[1], Ki-Suk Lee[1], Dae-Eun Jeong[1], Youn-Seok Choi[1], Young-Sang Yu[1], Dong-Soo Han[1], Andreas Vogel[2], Lars Bocklage[2], Guido Meier[2], Mi-Young Im[3], Peter Fischer[3] & Sang-Koog Kim[1]

[1]National Creative Research Center for Spin Dynamics & Spin-Wave Devices, and Nanospinics Laboratory, Department of Materials Science and Engineering, Seoul National University, Seoul 151-744, Republic of Korea, [2]Institut fu¨r Angewandte Physik und Zentrum fu¨r Mikrostrukturforschung, Universita¨t Hamburg, 20355 Hamburg, Germany, [3]Center for X-ray Optics, Lawrence Berkeley National Laboratory, Berkeley CA 94720, USA.

A wide variety of coupled harmonic oscillators exist in nature. Coupling between different oscillators allows for the possibility of mutual energy transfer between them and the information-signal propagation. Low-energy input signals and their transport with negligible energy loss are the key technological factors in the design of information-signal processing devices. Here, utilizing the concept of coupled oscillators, we experimentally demonstrated a robust new mechanism for energy transfer between spatially separated dipolar-coupled magnetic disks - stimulated vortex gyration. Direct experimental evidence was obtained by a state-of-the-art experimental time-resolved soft X-ray microscopy probe. The rate of energy transfer from one disk to the other was deduced from the two normal modes' frequency splitting caused by dipolar interaction. This mechanism provides the advantages of tunable energy transfer rates, low-power input signals and negligible energy loss in the case of negligible intrinsic damping. Coupled vortex-state disks might be implemented in applications for information-signal processing.

The magnetic vortex structure is very stable as the ground state in nanoscale magnetic elements[1,2]. It is characterized by an in-plane curling magnetization (chirality) around and an out-of-plane magnetization (polarization) in the central (core) region. In isolated disks, applied magnetic fields or spin currents induce vortex excitations, among which a translational mode[3–7] exists in which the vortex core rotates around its equilibrium position at a characteristic eigenfrequency (n_0 5 v_0/2p)[8] typically ranging from several hundred MHz to ,1 GHz. This so-called oscillatory gyrotropic motion occurs because the gyroforce of the vortex core is in balance with the restoring force acting on it, both of which forces are due to the competition between the short-range exchange and long-range dipolar interactions[8,9]. The rotational sense of the vortex gyration is determined by the polarization p (Refs. 4, 8) and thus is controllable by the p reversal, where p 5 11 (21) corresponds to the upward (downward) orientation of the magnetizations in the core. When the angular frequency of a driving force is close to v_0, the vortex-core motion and its switching can resonantly be driven even with low power consump-tion[10–12]. Such a vortex oscillation in the linear regime functions analogously to a simple harmonic oscillator. Recently the vortex structure is attracting keen interest owing to its potential application to nano-oscillators that emit microwave signals[9,13].

Moreover, individual vortex oscillators in two physically separated magnetic disks can be coupled via their magnetostatic interaction[14–20]. A displaced vortex core and its motion in one disk generate dynamically rotating stray fields, consequently affecting the potential energy of the other disk, in which vortex gyrations can be stimulated resonantly, and thus affecting each other. The relative vortex-core displacements in both disks as well as the disk-to-disk interdistance modify the interaction strength. These behaviours are analogous to those of coupled harmonic oscillators such as coupled pendulums or capacitively-coupled inductor-capacitor resona-tors[21]. Under the free-relaxation condition of such coupled oscillators, the kinetic and potential energy of one oscillator can be transferred to the other[21].

In the present study, we demonstrated reliably controllable dipolar-coupled vortex-core oscillations by a direct experimental observation of a complete energy transfer and all of the collective normal modes. This mechanism is a robust means of tunable energy transfer and information-signal transport between physically separated magnetic disks, and provides for the advantages of negligible-loss energy transfer and low-power input signals using the resonant vortex excitations.

Results

Experimental observation of vortex gyrations in dipolar-coupled vortex oscillators. Figure 1 shows the sample, which contains several two-disk pairs, each of which consists of two Permalloy (Py: $Ni_{80}Fe_{20}$) disks of the same dimensions. Note that both disks are positioned on the x axis, which is referred to as the bonding axis. The dipolar interaction between the two disks along this axis breaks the radial symmetry of the potential well of isolated disks. Applying a pulse current of 90 ns width and 2.5 ns rise and fall time along a single-strip Cu electrode (along the y axis) placed on only one disk (here

denoted as disk 1), we shifted the core position in disk 1 to ,165 nm in the 1y direction from the center position (x_1, y_1) 5 (0,0), and then allowed it to relax after turning off the field generated by the current pulse. During this free relaxation, the dynamics of the vortex gyrations in both disks of each pair were observed simultaneously, using spatiotemporal-resolved full-field magnetic transmission soft X-ray microscopy (MTXM). The magnetic contrast was provided via X-ray magnetic circular dichroism (XMCD) at the Fe L_3 edge (,707 eV). Measurements were made on the basis of a stroboscopic pump-and-probe technique[18,22,23] (see Supplementary A for details). In our earlier work[18], the microscope of 70 ps temporal and 20 nm spatial resolution was used to resolve the phases and amplitudes of both vortex-core positions, for the purpose of a feasibility test of such a state-of-the-art experiment. Figure 1b shows the two pairs studied, that is, d_{int}/(2R) 5 1.05 and 1.10, and

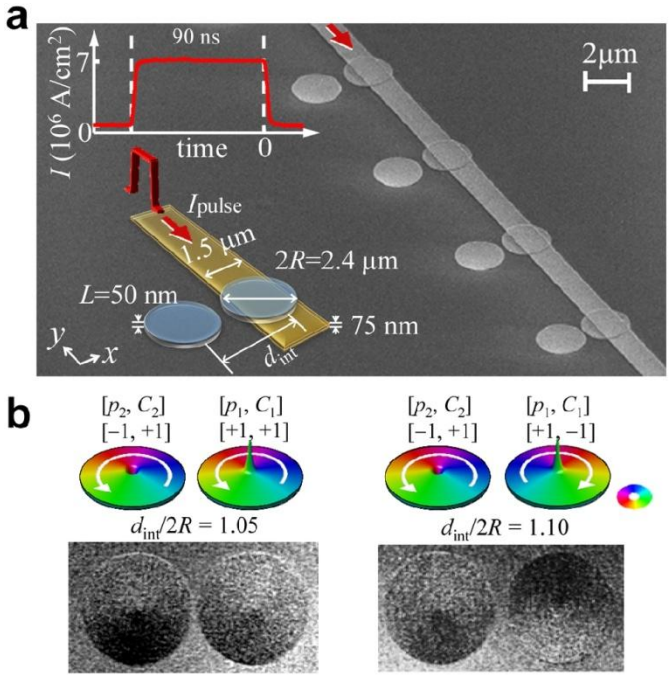

Figure 1 | Sample geometry of pairs of two vortex-state disks and initial ground states. (a) Scanning electron microscopy image of sample containing several two-disk pairs. Each pair contains two Permalloy (Py: $Ni_{80}Fe_{20}$) disks of the same dimensions, as indicated in the inset. The center-to-center distance normalized by diameter d_{int}/(2R) varies, such that d_{int}/(2R) 5 1.05, 1.1, 1.15, 1.2. Each pair is separated 5.6 mm from the neighbouring pairs. The insets show schematic illustrations of the sample with the indicated dimensions and the employed current pulse of 90 ns width, 2.5 ns fall-and-rise time, and 7.0310^6 A/cm^2 current density. (b) Fe L_3 edge XMCD images of both disks for two pairs, d_{int}/(2R) 5 1.05 and 1.10, the states are represented by perspective-view simulation results, as indicated includes simulation-perspective images of the initial vortex ground states in both disks. For the other pairs having larger d_{int}/(2R) values, the gyrations in disk 2 were difficult to observe, due to the small deviation of the vortex core from the center position, caused by the rapidly reduced interaction strength.

Figure 2 shows the experimental data on the vortex gyrations in the two disks in both pairs: d_{int}/(2R) = 1.05 and 1.10 in (a) and (b), respectively (see also Supplementary Movies. 1 and 2). Representative serial snapshot images of the XMCD contrasts are shown in each top panel. The trajectory curves of the motions of both vortex-core position vectors, X_1 = (x_1, y_1) and X_2 = (x_2, y_2), are plotted in the lower-right panels together with, in the lower-left panels, their oscillatory x and y components. Since a quasi-static local magnetic field (a pulse of sufficient length: here, 90 ns) was applied only to disk 1, the core position in that disk was shifted to (x_1, y_1) = (0, 165 nm) for [p_1, C_1] = [1, 1] and to (x_1, y_1) = (0, 165 nm) for [p_1, C_1] = [+1, -1]. The opposite sign of the y displacement in disk 1 between d_{int}/(2R) = 1.05 and 1.10 is attributable to the opposite chirality of disk 1 in the two pairs. Once the pulse field was turned off (at t = 0, the reference), the vortex core in disk 1 began to gyrate with decreasing oscillation amplitude starting from (x_1, y_1) =(0, 165 nm), whereas the vortex core in disk 2 began to gyrate with increasing oscillation amplitude starting from (x_2, y_2) = (0, 0). The vortex core in disk 1 gyrated counter-clockwise, indicating the upward core (p_1 5 11) orientation, whereas the vortex core in disk 2 gyrated clockwise, corresponding to the downward core (p_1 = -1) orientation (see Fig. 2a). Figure 2b shows similar characteristic oscillations of the given vortex state configuration. Micromagnetic simulation results (see Methods) are in excellent agreements with the experimental one, except for small discrepancies of their frequencies and absolute amplitudes. Experimental results show smaller oscillation amplitudes and frequencies, which might be attributed to the imperfection of the sample and weaker interaction between both disks due to a possible reduction in the saturation magnetization of the sample.

Energy transfer between two dipolar-coupled vortex oscillators.

The most important finding here is that the vortex-core gyration in disk 2 is stimulated by the vortex-core gyration in disk 1,

not by externally applied pulse fields, but rather through the magneto-static interaction between the two disks. For the case of $d_{int}/(2R) = 1.05$, the decreasing amplitude in disk 1 started to increase again at the time t = 26 ns, whereas the increasing amplitude in disk 2 began to decrease (see Fig. 2a). For $d_{int}/(2R) = 1.10$, the amplitude decay in disk 1 occurs at a longer time, t = , 45 ns (see Fig. 2b). Since the magnetic potential energy of a vortex depends on the displacement of the vortex core from the disk center[8], a complete energy transfer between dipolar-coupled vortex-state disks can be observed directly, via the variations of the displacements of both vortex cores, that is, $|X_1|$ and $|X_2|$, as shown in Fig. 3. Such a crossover in the vortex-core gyration modulation envelope between disks 1 and 2 confirms that the energy stored via the displaced core by an input-signal pulse field is transferred from disk 1 to disk 2 through the robust mechanism of stimulated vortex gyration in dipolar-coupled vortex oscillators. The high efficiency of this energy transfer mechanism is evidenced by the low (almost zero) amplitudes at the nodes of the beating pattern of the coupled vortex oscillators. Note that the mismatch between the nodes of the vortex-gyration amplitude in one disk and the anti-nodes in the other disk results from the intrinsic damping of a given material (see Supplementary B).

The total energy of undamped coupled oscillators, which is the sum of the first and second oscillator energies and the interaction energy between the oscillators, is constant. Magnetic vortices typically reside in potentials, which give rise to corresponding eigen-frequencies up to , 1 GHz. However, in principle these frequencies can be modified virtually in any desired frequency range , which is an important and advantageous aspect of the application of coupled vortex oscillators. As in every coupled harmonic oscillator system, the original resonance frequency of the non-interacting oscillator is either enhanced

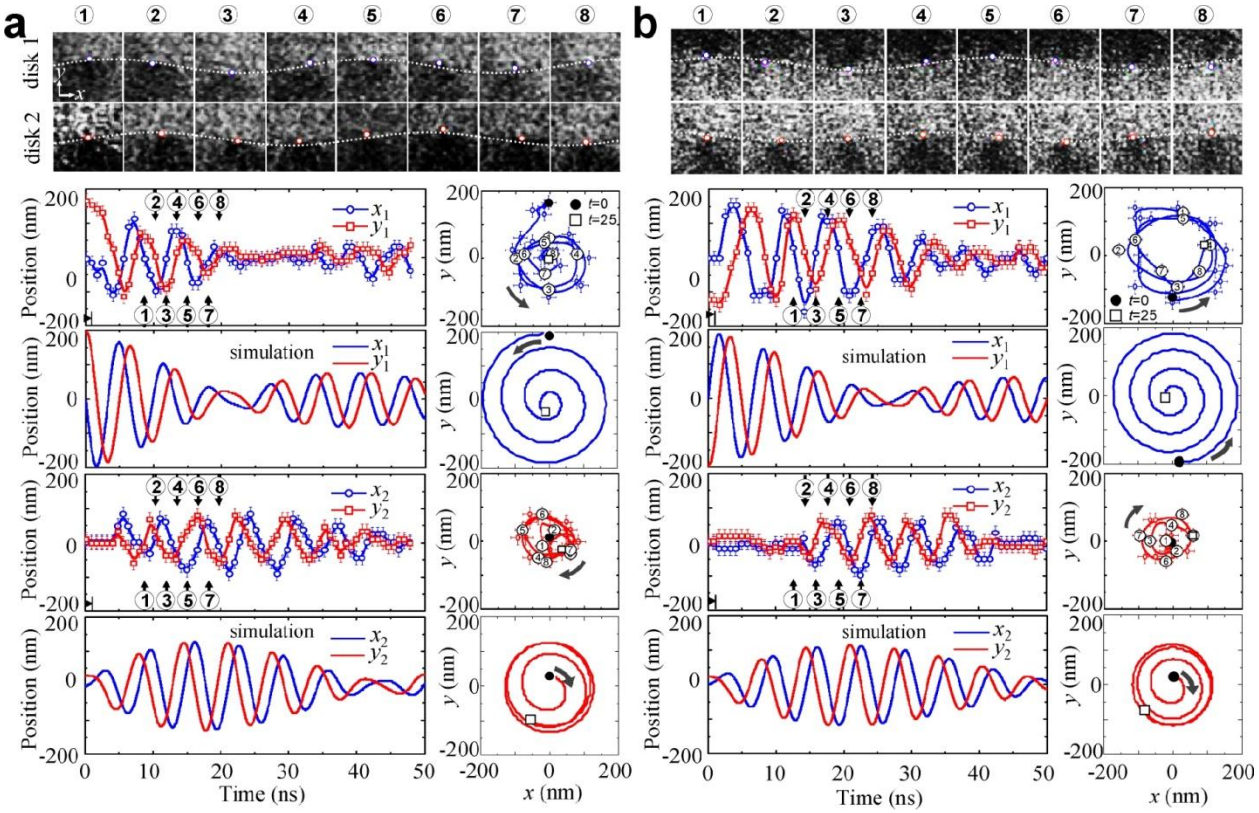

Figure 2 | MTXM observation of vortex-core gyrations in dipolar-coupled Py disks for $d_{int}/(2R)$ 5 1.05 in (a) and 1.10 in (b), compared with the corresponding simulation results. In each of a and b, the first row, are serial snapshot XMCD images of temporal evolution of vortex-core gyrations, starting from t 5 8.8 ns ( ) and ending at t 5 19.7 ns ( ) for a), and starting from t 5 12.5 ns ( ) and ending at t 5 24.2 ns ( ) for b). In each of a) and b), the second (disk 1) and fourth (disk 2) row are experimental results of the x and y components of vortex-core positions (left) from center position (x, y) 5 (0,0), and constructed vortex-core trajectories (right). The third and fifth row indicate the corresponding simulation results.

or reduced by the coupling[21]. Generally a symmetric and an antisymmetric mode having a lower and a higher frequency compared with the original eigenfrequency in uncoupled disks, respectively, appear. The frequency splitting between the symmetric and antisymmetric modes have a direct correlation with the interaction energy, and can be deduced from the beating pattern of coupled oscillations (see Supplementary B). It is clear that such a modulation envelope crossover between disks 1 and 2, as demonstrated in Figs. 2 and 3, is the result of the superposition of two equally weighted normal modes of different frequencies excited in a given dipolar-coupled oscillator system. We assume that all of the experimental results are within the linear regime. The beating frequency $\Delta\omega$ of the modulation envelope functions in disk 1 and disk 2 can be obtained by fitting the data of $|\mathbf{X}_1|$ and $|\mathbf{X}_2|$ to two orthogonal sinusoidal functions with an attenuation term, $|\mathbf{X}_1| = |A\cos(\Delta\omega t/2)|\exp(-\beta t)$ and $|\mathbf{X}_2| = |A\sin(\Delta\omega t/2)|\exp(-\beta t)$: $\Delta\omega/2\pi$ = 20 MHz and 12 MHz for $d_{int}/(2R)$ = 1.05 and 1.10, respectively. These results agree well on the fact that this angular frequency splitting $\Delta\omega$ takes place according to interaction between oscillators in a coupled system (see Supplementary C) and the magnitude of $\Delta\omega$ varies with the interdistance between neighbouring oscillators.

Another important parameter is β, which represents the energy loss during vortex-gyration-mediated signal propagation through the neighbouring disks. Based on Thiele's equation of vortex-core motion, the attenuation parameter is expressed analytically as $\beta = -(D/G)\omega_0$ for an isolated disk with the gyrovector constant G and the damping constant D (Ref. 24). This parameter can be rewritten as $\beta = \frac{1}{2}\alpha[2 + \ln(R/R_c)]\omega_0$ with the intrinsic Gilbert damping constant α and the vortex-core radius $R_c = 0.68L_{ex}(L/L_{ex})^{1/3}$ where the disk thickness L and the exchange length $L_{ex} = \left(2A_{ex}/M_s^2\right)^{1/2}$ with the exchange stiffness A_{ex} and the saturation magnetization M_s. For the case of experimentally obtained value of α = 0.01 ± 0.002 (Refs. 25–27) for a given Py material and the eigenfrequency $\omega_0 = 2\pi \times (157 \pm 3)$ MHz for isolated Py disks of R = 1.2 μm and L = 50 nm (see Methods), the value of $\beta = 2\pi \times (4.81\pm1.05)$ MHz is found to be in good agreement with the values of β , $2\pi \times (4.2 \pm 0.7)$ MHz and $2\pi \times (3.0 \pm 0.7)$ MHz for $d_{int}/(2R)$ = 1.05 and 1.10, respectively, which are obtained from fits to the experimental data shown in Fig. 3. Such good agreements are strong proof that energy loss through vortex-gyration-mediated signal transfer is determined by the intrinsic damping constant and dimensions of a given material. This means that further reduction of attenuation can be achieved by material engineering. For example, for a relatively low intrinsic damping constant**,** α = 0.0023 for NiMnSb, β is reduced drastically to $2\pi \times (0.8\pm0.1)$ MHz (**s**ee Supplementary D). Some Heusler alloys are reported to have extremely small values of α*,* for instance, α = 0.00006 for Co_2MnSi as found from an *ab initio* calculation[28] and α = 0.001 for Co_2FeAl as obtained from ferromagnetic resonance measurement[29].

Normal modes representation of coupled vortex oscillations

To directly obtain the value of $\Delta\omega$ from the experimentally observed vortex gyrations in the coupled system, we transformed the x and y component oscillations in each disk into two normal-mode oscillations on the basis of normal-mode coordinates $(N1_X, N1_Y) = (x_1+x_2, y_1-y_2)$ and $(N2_X, N2_Y) = (x_1-x_2, y_1+y_2)$ for the case of $p_1p_2 = -1$. In the normal-mode representation, the experimentally observed vortex gyrations in real coordinates (x, y) were decoupled into two normal modes having corresponding single dominant frequencies, as shown in Fig. 4 (see also the two normal modes for a different value, $d_{int}/(2R) = 1.10$, in Supplementary E). Figures 4a reveals that the two normal modes were excited almost equally and that their amplitudes were damped monotonically, as in free-relaxation vortex-core gyrations in uncoupled disks. According to their FFT spectra in Fig. 4b, the lower and higher eigenfrequencies for the two normal modes were 145 ± 10 and 165 ± 10 MHz, and thus, their frequency splitting was $\Delta\omega/2\pi$ = 20 MHz for $d_{int}/2R$ = 1.05, which is in excellent agreement with the values obtained from the fit to the modulation envelope functions of $|\mathbf{X}_1|$ and $|\mathbf{X}_2|$ with the corresponding damping (Fig. 3).

Figure 4: **Normal-mode representations of vortex-core gyrations in dipolar-coupled oscillators for $d_{int}/(2R) = 1.05$.**

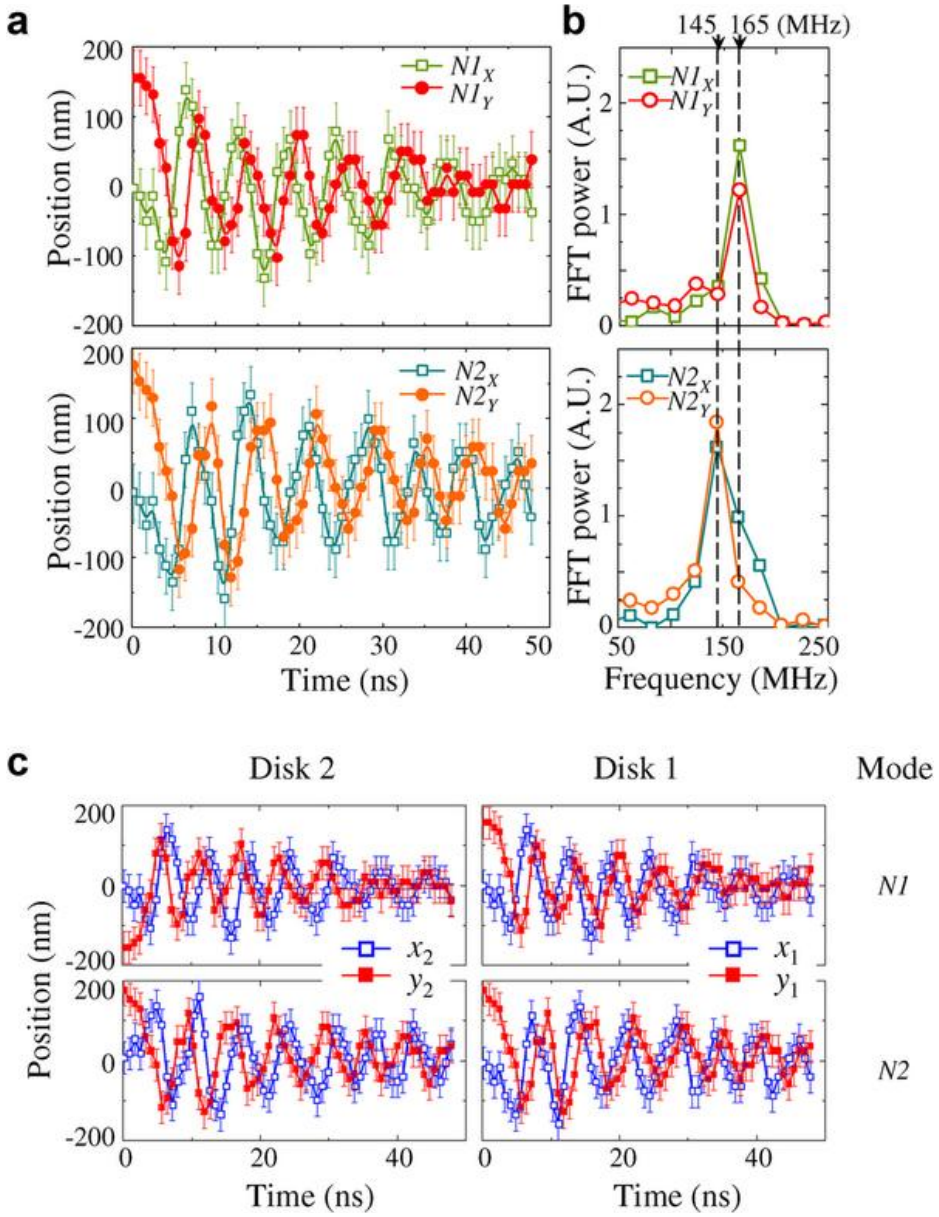

(a) Oscillatory core motions and (b) dominant frequency spectra. The two normal-mode coordinates are represented as ($N1_X = x_1+x_2$, $N1_Y = y_1-y_2$) and ($N2_X = x_1-x_2$, $N2_Y = y_1+y_2$), corresponding to their trajectory curves and FFT spectra. c, The *x* and *y* positions of vortex-core oscillations in each disk for each normal mode (see the text).

Moreover, we can decompose coupled vortex gyrations into the two normal modes of each disk with respect to the ordinary coordinates according to the relations of $(x_1, y_1)_{N1} = \frac{1}{2}(N1_X, N1_Y)$, $(x_1, y_1)_{N2} = \frac{1}{2}(N2_X, N2_Y)$, $(x_2, y_2)_{N1} = \frac{1}{2}(N1_X, -N1_Y)$, and $(x_2, y_2)_{N2} = \frac{1}{2}(-N2_X, N2_Y)$. Figure 4c shows that for the higher-frequency *N1* mode, the *x* positions of the vortex-core motions in both disks oscillate in-phase but their *y* positions do so out-of-phase, and vice-versa for the lower-frequency *N2* mode. Since the vortex-core motion in one disk in the direction normal to the bonding axis (i.e., along the *y* axis) results in stronger stray fields (exciting vortex motion in the other disk) than it does along the bonding axis (the *x* axis), the dipolar interaction is dominated by the relative *y* position of vortex-core motions between the two disks. Thus, the interaction energy of the *N1* mode having out-of-phase oscillation at the *y* positions is higher than that of the *N2* mode having in-phase oscillation at the *y* position. Analogous to a general coupled harmonic oscillator, the *N1* mode with the antisymmetric *y* component oscillation *works harder* than the *N2* mode with the symmetric one. As the result, the frequency of the *N1* mode is higher than that of the *N2* mode, as noted earlier. More generally, in two dipolar-coupled disks with arbitrary *p*- and *C*–configuration states, the mode characterized by out-of-phase oscillation between C_1y_1 and C_2y_2 is higher-frequency antisymmetric, whereas that with in-phase oscillation is lower-frequency symmetric. This is owed to the fact that the interaction energy of each mode is determined by the

relative *C* configuration between coupled vortices, which energy is itself determined by the *C*–dependent direction of the stray fields induced by vortex-core shifts.

Energy exchange rate and its dependence on interdistance

The energy exchange rate τ_{ex} between oscillators is technologically important from the information-signal transport point of view. It is determined by the coupling strength. Let τ_{ex} be the time period required for transferring the potential energy stored in disk 1 (here, due to the initial vortex-core shift) completely to disk 2. The value of τ_{ex} can be estimated from the frequency splitting determined from the modulation envelopes of $|\mathbf{X}_1|$ and $|\mathbf{X}_2|$, (see Supplementary F) and consequently, is given as half of the modulation envelope period, $\frac{1}{2}(2\pi/\Delta\omega)$, so that τ_{ex} = 26 ± 3 ns and 45 ± 6 ns for $d_{int}/(2R)$ = 1.05 and 1.10, respectively. Since the strength of the interaction between two vortices determines the frequency splitting of dipolar-coupled vortices, a smaller value of τ_{ex} can be obtained by increasing the strength of the dipolar interaction. For any given material and vortex state, it is known that the dipolar interaction between two vortices depends strongly on the interdistance between them[14, 15]. This was confirmed by the present experiments. Also, the micromagnetic simulation data (see Supplementary G) clearly show that the value of τ_{ex} varies with the interdistance as $\tau_{ex} \sim (d_{int}/2R)^{-3.91\pm0.07}$. Accordingly, the energy transfer rate between vortex-state disks is tunable varying their interdistance.

Energy exchange rate depending on relative vortex polarization configuration

It is worth noting that the relative motion of the vortex-core gyration of two vortices also affects the strength of their interactions: the dipolar interaction of vortex-core gyrations having opposite rotational senses due to opposite polarities is much stronger than that of gyrations having the same rotational sense due to the same polarity. From the simulation (see Supplementary H), τ_{ex} for the opposite polarity is ~ 2 times faster than that for the same polarity. Since the magnetostatic interaction strength depends directly on the stray field of each disk, thus, the larger the saturation magnetization is, the stronger will be the interaction strength, yielding faster τ_{ex} and hence faster signal transport. Because the polarity of a given vortex can be manipulated in a controllable manner by applying rotating or pulse fields locally to that vortex state using specially designed electrodes, as reported in Refs. [30–31], the polarities of vortices can be one of the crucial parameters for governing the interaction strength of energy transfer, and hence the exchange rate.

To conclude, we experimentally observed, by time-resolved MTXM, energy and information-signal transfer via stimulated vortex gyration through dipolar interaction between separated magnetic disks. This robust new mechanism for energy transfer provides the advantages of a fast and tunable energy transfer rate that is a function of disk interdistance and interaction strength. Control of energy loss during gyration-mediated signal transfer is possible with material engineering; in fact, almost lossless energy transfer can be achieved by employment of a material having negligible damping. Vortex gyration also can be achieved with low-power consumption through the resonant vortex excitation. This finding opens a new avenue to the development of energy efficient information processing devices such as logic gates based on vortex-state networks.

Sample preparation

The sample shown in Fig. 1 was prepared on a 100 nm-thick silicon nitride membrane by electron-beam lithography, thermal evaporation, and lift-off processing. The two disks in each pair have a different center-to-center interdistance, such that $d_{int}/2R$ = 1.05, 1.1, 1.15, and 1.2, and each pair is separated at a sufficiently large distance, 5.6 μm, from neighbouring pairs. A single-strip Cu electrode leads to strong local fields, as shown in Supplementary I, so that local excitations of the vortex, in each pair, are possible only in disk 1. Note that we confirmed that such local fields do not allow for vortex excitations in disk 2 positioned sufficiently far from the electrode stripline, in any of the $d_{int}/2R$ cases studied here. The eigenfrequency of the vortex gyrations in isolated Py disks, by ferromagnetic resonance measurements performed on an array of Py disk pairs of the same dimensions and d_{int} / 2R = 1.56, was determined to be around 157 ± 3 MHz.

Micromagnetic simulation

We performed micromagnetic simulations of coupled vortex gyrations under free relaxation for two Py disks of the same dimensions as those of the sample for $d_{int}/(2R)$ = 1.05 and 1.10. To mimic the experimental conditions, we used the same initial vortex-state configurations as those of the real sample. The material parameters for Py are as follows: the exchange stiffness A_{ex} = 13 pJ/m, the saturation magnetization M_s = 7.2×10^5 A/m, and a zero magnetic anisotropy constant. The cell size was 4×4×50 nm^3 with the Gilbert damping constant α = 0.01. We used the OOMMF code that utilizes the Landau-Lifshitz-Gilbert equation of motion[32].

1 Shinjo, T., Okuno, T., Hassdorf, R., Shigeto, K. & Ono, T. Magnetic vortex core observation in circular dots of Permalloy. Science 289, 930–932 (2000).
2 Wachowiak, A. et al. Direct observation of internal spin structure of magnetic vortex cores. Science 298, 577–580 (2002).
3 Park, J. et al. Imaging of spin dynamics in closure domain and vortex structures. Phys. Rev. B 67, 020403 (2003).
4 Choe, S. B. et al. Vortex core-driven magnetization dynamics. Science 304, 420–

a. (2004).
5 Kasai, S. et al. Current-driven resonant excitation of magnetic vortices. Phys. Rev. Lett. 97, 107204 (2006).
6 Bolte, M. et al. Time-resolved x-ray microscopy of spin-torque-induced magnetic vortex gyration. Phys. Rev. Lett. 100, 176601 (2008).
7 Lee, K.-S. & Kim, S.-K. Two circular-rotational eigenmodes and their giant resonance asymmetry in vortex gyrotropic motions in soft magnetic nanodots. Phys. Rev. B 78, 014405 (2008).
8 Guslienko, K. Y. et al. Eigenfrequencies of vortex state excitations in magnetic submicron-size disks. J. Appl. Phys. 91, 8037–8039 (2002).
9 Dussaux, A. et al. Large microwave generation from current-driven magnetic vortex oscillators in magnetic tunnel junctions. Nat. Commun. 1:8, doi: 10.1038/ ncomms1006 (2010).
10 Waeyenberge, B. et al. Magnetic vortex core reversal by excitation with short bursts of an alternating field. Nature 444, 461–464 (2006).
11 Yamada, K. et al. Electrical switching of the vortex core in a magnetic disk. Nature Mater. 6, 269–273 (2007).
12 Kim, S.-K., Lee, K.-S., Yu, Y.-S. & Choi, Y.-S. Reliable low-power control of ultrafast vortex-core switching with the selectivity in an array of vortex states by in-plane circular-rotational magnetic fields and spin-polarized currents. Appl. Phys. Lett. 92, 022509 (2008).
13 Pribiag, V. S. et al. Magnetic vortex oscillator driven by d.c. spin-polarized current. Nature Phys. 3, 498–503 (2007).
14 Shibata, J., Shigeto, K. & Otani, Y. Dynamics of magnetostatically coupled vortices in magnetic nanodisks. Phys. Rev. B 67, 224404 (2003).
15 Vogel, A., Drews, A., Kamionka, T., Bolte, M. & Meier, G. Influence of dipolar Interaction on vortex dynamics in arrays of ferromagnetic disks. Phys. Rev. Lett. 105, 037201 (2010).
16 Barman, S., Barman, A. & Otani, Y. Dynamics of 1-D Chains of Magnetic Vortices in Response to Local and Global Excitations. IEEE Trans. Magn. 79, 1342–1345 (2010).
17 Barman, A., Barman, S., Kimura, T., Fukuma, Y. & Otani, Y. Gyration mode splitting in magnetostatically coupled magnetic vortices in an array. J. Phys. D: Appl. Phys. 43, 422001 (2010).
18 Jung, H. et al. Observation of coupled vortex gyrations by 70-ps-time- and 20-nm-space-resolved full-field magnetic transmission soft x-ray microscopy. Appl. Phys. Lett. 97, 222502 (2010).
19 Vogel, A. et al. Coupled vortex oscillations in spatially separated permalloy squares, Phys. Rev. Lett. 106, 137201 (2011).
20 Sugimoto, S. et al. Dynamics of coupled vortices in a pair of ferromagnetic disks, Phys. Rev. Lett. 106, 197203 (2011).
21 Thornton, S. T. & Marion, J. B. Classical dynamics of particles and systems, Fifth Ed.(Thomson, 2004).
22 Bocklage, L. et al. Time-resolved imaging of current-induced domain-wall oscillations. Phys. Rev. B 78, 180405(R) (2008)
23 Fischer, P. Soft X-ray microscopy –a powerful analytical tool to image magnetism down to fundamental length and time scales. AAPPS bulletin 18(6), 12–17 (2008).
24 Guslienko, K. Y. Low-frequency vortex dynamic susceptibility and relaxation in mesoscopic ferromagnetic dots. Appl. Phys. Lett. 89, 8037–8039 (2002).
25 Hiebert, W. K., Stankiewicz, A., & M. R. Freeman Direct Observation of Magnetic Relaxation in a Small Permalloy Disk by Time-Resolved Scanning Kerr Microscopy. Phys. Rev. Lett. 79, 1134–1137 (1997).
26 Gerrits, Th. et al. Magnetization dynamics in NiFe thin films induced by short in-plane magnetic field pulses. J. Appl. Phys. 89, 7648–7650 (2001).
27 Sandler, G. M., Bertram, H. N., Silva, T. J., & Crawford, T. M. Origins of the damping constant in thin NiFe films. J. Appl. Phys. 85, 5080–5082 (1999).
28 Liu, C. et al. Origin of low Gilbert damping in half metals. Appl. Phys. Lett. 95, 022509 (2009).
29 Mizukami, S. et al. Low damping constant for Co2FeAl Heusler alloy films and its correlation with density of states. J. Appl. Phys. 105, 07D306 (2009).
30 Yu, Y.-S., Jung, H., Lee, K.-S., Fischer, P., Kim, S.-K. Memory-bit selection and recording by rotating fields in vortex-core cross-point architecture. Appl. Phys. Lett. 98, 052507 (2011).
31 Weigand, M. et al. Vortex core switching by coherent excitation with single in-plane magnetic field pulses. Phys. Rev. Lett. 102, 077201 (2009).
32 Donahue, M. & Porter, D. OOMMF User's Guide, Version 1.0. Interagency Report NISTIR 6376. National Institute of Standards and Technology, (1999).

Acknowledgments

1.
This research was supported by the Basic Science Research Program through the National Research Foundation of Korea (NRF), funded by the Ministry of Education, Science, and Technology (Grant No. 20110000441). The operation of the microscope was supported by the Director, Office of Science, Office of Basic Energy Sciences, Materials Sciences

and Engineering Division, of the U.S. Department of Energy. Financial support of the Deutsche Forschungsgemeinschaft via the SFB 668 ‘‘Magnetismus vom Einzelatom zur Nanostruktur’’ and via the Graduiertenkolleg 1286 ‘‘Functional Metal-Semiconductor Hybrid Systems’’ is gratefully acknowledged, as is that of the City of Hamburg via Cluster of Excellence ‘‘Nano-Spintronics.’’

Author contributions

H.J. and K.-S.L. contributed equally to this work. S.-K.K conceived the main idea and the conceptual design of the experiments, together with H.J., K.-S.L., A.V., and G.M., H.J., K.-S.L, and D.-S.H. performed micromagnetic simulations. A.V., L.B., and H.J. prepared the samples. H.J., K.-S.L., Y.-S.Y., Y.-S.C., A. V., L.B, M.-Y.I., P.F., and S.-K.K. performed the x-ray imaging experiments. H.J., K.-S.L., D.-E.J., A.V., G.M and S.-K.K. contributed to the interpretations of the experimental data. S.-K.K and G.M. led the project and wrote the manuscript together with H.J., K.-S.L., A.V., and P.F.

DISCLAIMER

This work was supported by the Director, Office of Science, of the U.S. Department of Energy under Contract No. DE-AC02-05CH11231.